# The Effect of Incomplete Surface Accommodation on Heat Transfer and Drag of Truncated Wedges in the Rarefied Regime

**Wilson F. N. Santos**
Combustion and Propulsion Laboratory
National Institute for Space Research
Cachoeira Paulista, SP 12630-000
Wilson@lcp.inpe.br

***Abstract.*** *This work describes a computational study on hypersonic flow past truncated wedges at zero incidence. Effects of incomplete surface accommodation in rarefied flow on the aerothermodynamic surface quantities have been investigated by employing the Direct Simulation Monte Carlo Method in combination with the Cercignani-Lampis-Lord gas-surface interaction model, which incorporates separate accommodation coefficients for normal and tangential velocity components. The work focuses the attention of designers of hypersonic configurations on the fundamental parameter of bluntness, which can have an important impact on even initial design. The results presented highlight the sensitivity of the heat transfer and drag coefficients to changes on the gas-surface accommodation coefficients. It was found that the heat transfer and drag coefficients decreased by a reduction on the tangential accommodation coefficient.*

***Palavras-chave:*** *DSMC, Hypersonic Flow, Rarefied Flow, Incomplete Surface Accommodation.*

## 1. INTRODUCTION

An increasingly important problem in aerospace engineering is that of predicting aerodynamic characteristics of vehicles flying at very high speeds and high altitudes. Under this conditions the flow about a given aerodynamic configuration may be sufficiently rarefied that the appropriate molecular mean free path becomes too large, compared to a characteristic length of the vehicle for the use of continuum assumptions but not large enough for the use of the free molecular theory. In such an intermediate or transition rarefied gas regime, the complete investigation of the flowfield structure would require the full formulation of kinetic theory. The governing equation in the transition regime is the Boltzmann equation (Cercignani, 1988). Nevertheless, in order to circumvent the difficult of a direct solution of the Boltzmann equation, the Direct Simulation Monte Carlo (DSMC) method (Bird, 1994) has been the appropriate choice for problems involving flows of rarefied hypersonic aerothermodynamics.

One of the key issues concerning hypersonic configurations is the leading edge of the vehicle. Hypersonic configurations are generally characterized by slender bodies and sharp leading edges in order to achieve good aerodynamic properties like high lift and low drag. Certain configurations, such as waveriders (Nonweiler, 1959), are designed analytically with infinitely sharp leading edges for shock wave attachment. Because the shock wave is attached to the leading edge of the vehicle, the upper and lower surfaces of the vehicle can be designed separately. Furthermore, the shock wave acts as a barrier in order to prevent spillage of higher-pressure airflow from the lower side of the vehicle to the upper side, resulting in a high-pressure differential and enhanced lift.

Usually, it is extremely difficult to construct a perfectly sharp leading edge. Any manufacturing error results in a significant deviation from the design contour. Moreover, sharp edges are difficult to maintain because they are easily damaged. Additionally, because heat transfer increases

inversely with the leading edge radius, high heating is associated with sharp edges. Therefore, for practical hypersonic configurations, leading edges should be blunt for heat transfer, manufacturing and handling concerns. Because blunt leading edge promotes shock wave standoff, practical leading edges will have shock detachment, making leading edge blunting a major concern in the design and prediction of flowfields over hypersonic configurations.

The flowfield properties upstream the leading edge of a body are affected by molecules reflected from the edge region. The degree of the effect is in part conditioned by the edge geometry. In this context, Santos (2002) and Santos (2004) investigated the effect of the leading edge thickness on the flowfield structure and on the aerodynamic surface quantities over truncated wedges. The thickness effect was examined for a range of Knudsen number, based on the thickness of the flat face, covering from the transitional flow regime to the free molecular flow one. The emphasis of the work was to provide a critical analysis on maximum allowable geometric bluntness, dictated by either handling or manufacturing requirements, resulting on reduced departures from ideal aerodynamic performance of the vehicle. Thus allowing the blunted leading edge to more closely represent the original sharp leading edge flowfield. Such analysis is also important when a comparison is to be made between experimental results in the immediate vicinity of the leading edge and the theoretical results, which generally assume a zero-thickness leading edge. Santos (2003) extended further the analysis presented by Santos (2002) on truncated wedges by performing a parametric study on these shapes with emphasis placed on the compressibility effects. The primary goal was to assess the sensitivity of the shock wave standoff distance, stagnation point heating and total drag to changes in the freestream Mach number.

These works (Santos, 2002 and Santos, 2003) on hypersonic flow past truncated wedges have been concentrated primarily on the analysis of the aerothermodynamic surface quantities by considering the diffuse reflection model as being the gas-surface interaction. The diffuse model assumes that the molecules are reflected equally in all directions, quite independently of their incident speed and direction. As a space flight vehicle is exposed to a rarefied environment over a considerable time, a departure from the fully diffuse model is observed, resulting from the colliding molecules that clean the surface of the vehicle, which becomes gradually decontaminated. Molecules reflected from clean surfaces show lobular distribution in direction. The flux distribution of scattered molecules emitted from clean surfaces frequently has a lobular shape that is centered about an angle, which tends to approach the specular angle for very high energies and/or low angle of attack.

Both the aerodynamic surface quantities and the state of the gas adjacent to the body surface are very sensitive to the assumptions used in the calculation concerning the gas-surface interaction model for transitional and free molecular flows. In addition, the essential phenomena of rarefied gases are found mostly in the region relatively near to the solid boundaries, i.e., within a few mean free paths. Thus the knowledge of the physics of the interaction of gas molecules and solid surfaces is of primary importance.

In an effort to obtain further insight into the nature of the aerodynamic surface quantities of truncated wedges under hypersonic transitional flow conditions, a parametric study is performed on these shapes with a great deal of emphasis placed on the gas-surface interaction effects. In this scenario, the primary goal of this paper is to assess the sensitivity of the heat transfer and drag coefficients to variations in the surface accommodation coefficients experienced by the leading edges by employing the Cercignani-Lampis-Lord (CLL) model (Lord, 1991a). The CLL model, which incorporates independent accommodation coefficients for the normal and tangential velocity components, is implemented into the DSMC code, and simulations are performed by assuming two-dimensional rarefied hypersonic flow.

## 2. GAS-SURFACE INTERACTION MODEL

The influence of the model of gas-surface interactions on the aerodynamic forces and heat transfer increases substantially as the gas rarefaction increases. As a result, a correct choice of the

model for calculating hypersonic rarefied flows plays an important role.

Three models of gas-surface interactions may be employed in the DSMC method: specular and diffuse interactions and some combination of these. In a specular reflection, molecules are reflected like a perfectly elastic sphere with reversal of the normal component of velocity and no change in either the parallel component of velocities and energy. In a diffuse reflection, the molecules are reflected equally in all directions usually with a complete thermal accommodation. The final velocity of the molecules is randomly assigned according to a half-range Maxwellian distribution determined by the wall temperature. The combination of diffuse reflection with specular reflection (Maxwell model) introduces a single parameter $f$ to indicate the fraction of those molecules reflected diffusely in a completely accommodated fashion according to a Maxwellian distribution corresponding to the wall temperature, and the remaining fraction (1-$f$), being assumed to reflect specularly.

The Maxwell model was followed by the introduction of three accommodation coefficients that describe the degree of accommodation of the incident normal momentum, tangential momentum and kinetic energy to those of the surface. The traditional definition (Schaaf and Chambre, 1961) for these coefficients is usually expressed as being,

$$\sigma_n = \frac{p_i - p_r}{p_i - p_w} \qquad \sigma_t = \frac{\tau_i - \tau_r}{\tau_i} \qquad \alpha_r = \frac{e_i - e_r}{e_i - e_w} \tag{1a, b, c}$$

where terms $p$, $\tau$ and $e$ refer to the momentum flux acting normal and tangential to the surface, and the energy flux to the surface per unit area per unit time, respectively; subscripts $i$ and $r$ stand for the incident and reflected components, and $w$ refers to the component that would be produced by a diffuse reflection at the temperature of the surface.

Data from many experiments show that molecules reflected or re-emitted from solid surfaces present lobular distributions under high vacuum conditions and are poorly represented by the Maxwell model. However, this model is widely used because it satisfies the principle of detailed balance or reciprocity. Detailed balance means that at equilibrium every molecular process and its inverse process must individually balance. A phenomenological model that satisfies detailed balance and has demonstrated improvement over the Maxwell model has been proposed by Cercignani and Lampis (1971) (CL model). This model is based on the definition of the accommodation coefficients $\alpha_n$ and $\alpha_t$ that represent the accommodation coefficients for the kinetic energy associated with the normal and tangential components of velocity. The CL model provides a continuous spectrum of behavior from specular reflection at one end to diffuse reflection with complete energy accommodation at the other, and produces physically realistic distributions of direction and energy re-emitted molecules. Lord (1991a) has shown that the CL model is suited for the DSMC method, and described how to incorporate it into the DSMC method. The DSMC method with Lord's implementation is referred as the Cercignani-Lampis-Lord (CLL) method. Figure 1 displays a schematic comparison of the Maxwell reflection model and the CLL reflection model. The CL model has also been extended for covering diffuse scattering with partial energy accommodation and for simulating the accommodation of vibrational energy of a diatomic molecule modeled as simple harmonic oscillator (Lord, 1991b) and an anharmonic oscillator (Lord, 1995).

In order to simulate the partial surface accommodation, the Cercignani-Lampis-Lord (CLL) model (Lord, 1991a) was included in this DSMC calculation. The CLL model is derived assuming that there is no coupling between the normal and tangential momentum components. The two adjustable parameters appearing in the CLL model are the normal component of translational energy $\alpha_n$ and the tangential component of momentum $\sigma_t$. However, in the implementation of the CLL model in the DSMC method, Bird (1994) has shown that it is equivalent to specify the normal $\alpha_n$ and tangential $\alpha_t$ components of translational energy, since $\alpha_t = \sigma_t\,(2\text{-}\sigma_t)$, and thus that $\sigma_t < \alpha_t$, assuming that $\sigma_t$ lies between 0 and 1. In the present simulations, $\alpha_n$ and $\sigma_t$ are used as being the two adjustable parameters. It is important to mention that in the CLL model the accommodation of

internal energy is allowed to be independent of the translational accommodation.

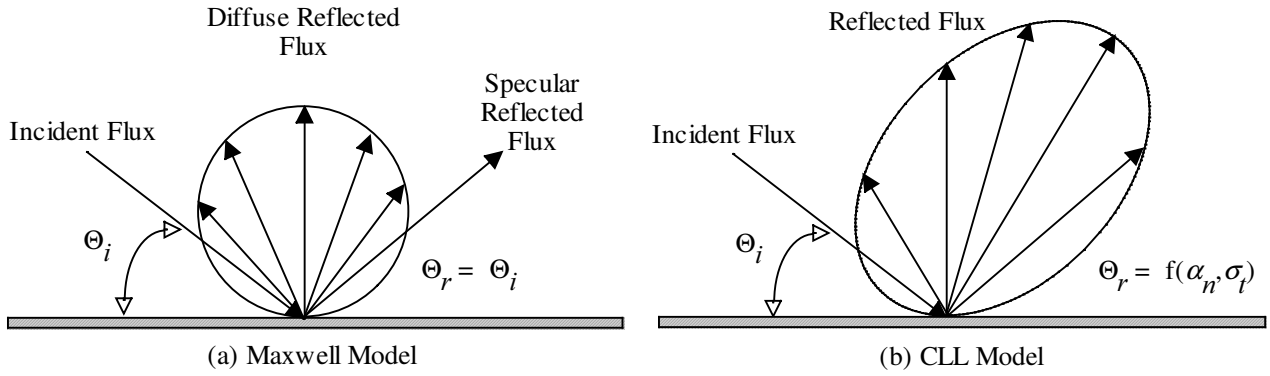


Figure 1. Drawing illustrating the Maxwell reflection model and the CLL reflection model.

## 3. LEADING EDGE GEOMETRY DEFINITION

The truncated wedges analyzed in this work are modeled by assuming a sharp leading edge of half angle $\theta$ with a circular cylinder of radius $R$ inscribed tangent to this sharp leading edge. The truncated wedges are also tangents to the sharp leading edge and the cylinder at the same common point. It was assumed a leading edge half angle of 10 degree, a circular cylinder diameter of $10^{-2}$m and truncated wedge thicknesses $t/\lambda_\infty$ of 0.01, 0.1 and 1, where $\lambda_\infty$ is the freestream mean free path. Figure (2a) illustrates schematically this construction. Since the wake region behind the truncated wedges is not of interest in this investigation, it was assumed that the truncated wedges are infinitely long but only the length $L$ is considered.

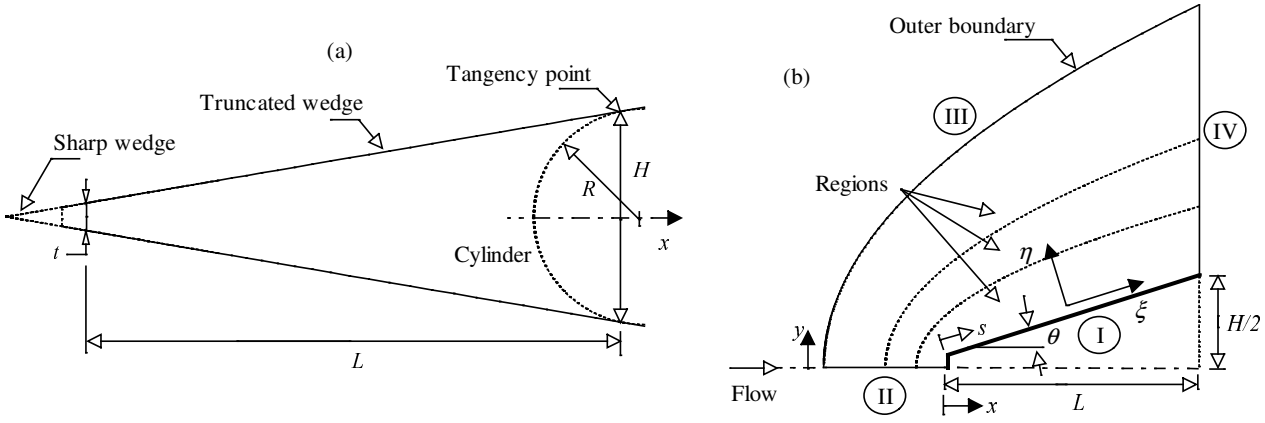


Figure 2: (a) Drawing illustrating the truncated wedge and (b) the computational domain.

## 4. COMPUTATIONAL METHOD AND PROCEDURE

It is well known that neither the continuum flow equations nor the collisionless flow equations are valid to predict leading edge aerothermodynamic characteristics throughout the transitional flow regime. During the last several years, the most successful numerical technique applied for computing leading edge flowfield and surface effects in the transitional flow regime has been the DSMC method pioneered by Bird (1994).

The DSMC method simulates real gas flows with various physical processes by means of a huge number of modeling particles, each of which is a typical representative of great number of real gas molecules. DSMC models the flow as being a collection of discrete particles, each one with a position, velocity and internal energy. The state of particles is stored and modified with time as the

particles move, collide, and undergo boundary interactions in simulated physical space.

The molecular collision kinetics are modeled by using the variable hard sphere (VHS) molecular model (Bird, 1981) and the no time counter (NTC) collision sampling technique (Bird, 1989). The energy exchange between kinetic and internal modes is controlled by the Borgnakke-Larsen statistical model (Borgnakke and Larsen, 1975), with internal energy exchange allowed only for rotation and vibration degrees of freedom. Simulations are performed using a non-reacting gas model consisting of two chemical species, $N_2$ and $O_2$.

In order to implement the particle-particle collisions, the flowfield is divided into a number of regions, which are subdivided into computational cells. The cell provides a convenient reference for the sampling of the macroscopic gas properties. The dimensions of the cells must be such that the change in flow properties across each cell is small. The linear dimensions of the cells should be small in comparison with the scale length of the macroscopic flow gradients normal to the streamwise directions, which means that the cell dimensions should be of the order of the local mean free path or even smaller (Bird, 1994). The cells are further subdivided into 4 subcells, 2 subcells/cell in each direction. The collision partners are selected from the same subcell for the establishment of the collision rate. Time is advanced in discrete steps such that each step ought to be sufficiently small in comparison with the local mean collision time (Bird, 1994).

The computational domain used for the calculation is made large enough so that body disturbances do not reach the upstream and side boundaries, where freestream conditions are specified. A schematic view of the computational domain is depicted in Fig. (2b). Advantage of the flow symmetry is taken into account, and molecular simulation is applied to one-half of a full configuration. Side I is defined by the body surface. Reflection with incomplete surface accommodation is the condition applied to this side. Side II is a plane of symmetry. In such a boundary, all flow gradients normal to the plane are zero. At the molecular level, this plane is equivalent to a specular reflecting boundary. Side III is the freestream side through which simulated molecules enter and exit. Finally, the flow at the downstream outflow boundary, side IV, is predominantly supersonic and vacuum condition is specified (Bird, 1994). At this boundary, simulated molecules can only exit.

Numerical accuracy in DSMC method depends on the grid resolution chosen as well as the number of particles per computational cell. Both effects were investigated to determine the number of cells and the number of particles required to achieve grid independence solutions. Grid independence was tested by running the calculations with half and double the number of cells in each direction compared to a standard grid. Solutions were near identical for all grids used and were considered fully grid independent.

The freestream and flow conditions used for the numerical simulation of flow past the wedges are those given by Santos (2002) and summarized in Tab. (1), and the gas properties (Bird, 1994) are shown in Tab. (2). The freestream velocity $V_\infty$ is assumed to be constant at 3.56 km/s, which corresponds to a freestream Mach number $M_\infty$ of 12. The translational and vibrational temperatures in the freestream are in equilibrium at 220 K, and the leading edge surface has a constant wall temperature $T_w$ of 880 K for all cases considered.

The overall Knudsen number $Kn$ is defined as the ratio of the molecular mean free path $\lambda$ in the freestream gas to a characteristic dimension of the flowfield. In the present study, the characteristic dimension was defined as being the thickness $t$ of the truncated leading edges. For the thicknesses investigated, $t/\lambda_\infty = 0.01$, 0.1 and 1, the overall Knudsen numbers corresponds to $Kn_t = 100$, 10, and 1. Finally, the Reynolds number $Re_t$ covers the range from 0.193 to 19.3, based on conditions in the undisturbed stream with leading edge thickness $t$ as the characteristic length.

In order to simulate the incomplete surface accommodation, the CLL model implemented in the DSMC code considered only the normal and tangential accommodation coefficients. The internal energy accommodation was kept equal to one for all calculations presented in this work. Hence, $\alpha_n$ and $\sigma_t$ are used as being the two adjustable parameters. The DSMC calculations were performed independently for three distinct numerical values for $\alpha_n$ and $\sigma_t$: 0.5, 0.75 and 1.0. $\alpha_n$ or $\sigma_t$ equal to 1.0 represents the diffusion reflection already investigated by Santos (2002).

Table 1. Freestream and flow conditions

| Temperature $T_\infty$ (K) | Pressure $p_\infty$ (N/m$^2$) | Density $\rho_\infty$ (kg/m$^3$) | Number density $n_\infty$ (m$^{-3}$) | Viscosity $\mu_\infty$ (Ns/m$^2$) | Mean free path $\lambda_\infty$ (m) |
|---|---|---|---|---|---|
| 220.0 | 5.582 | $8.753 \times 10^{-5}$ | $1.8209 \times 10^{21}$ | $1.455 \times 10^{-5}$ | $9.03 \times 10^{-4}$ |

Table 2. Gas properties

| | Mole fraction $X$ | Molecular mass $m$ (kg) | Molecular diameter $d$ (m) | Viscosity index $\omega$ |
|---|---|---|---|---|
| $O_2$ | 0.237 | $5.312 \times 10^{-26}$ | $4.01 \times 10^{-10}$ | 0.77 |
| $N_2$ | 0.763 | $4.65 \times 10^{-26}$ | $4.11 \times 10^{-10}$ | 0.74 |

## 5. COMPUTATIONAL RESULTS AND DISCUSSION

Attention is now focused on the calculations of the heat transfer and drag obtained from the DSMC results. The purpose of this section is to discuss and to compare differences in the profiles of these properties, expressed in coefficient form, due to variations on the normal and tangential accommodation coefficients associated to the gas-surface interaction.

### 5.1. Heat Transfer Coefficient

The heat flux $q_w$ to the body surface is calculated by the net energy flux of the molecules impinging on the surface. A flux is regarded as positive if it is directed toward the body surface. The net heat flux $q_w$ is related to the sum of the translational, rotational and vibrational energies of both incident and reflected molecules. The net heat flux is normalized by freestream kinetic energy flux $\frac{1}{2}\rho_\infty V_\infty^3$ and presented in terms of heat transfer coefficient $C_h$.

The effect of changing the normal $\alpha_n$ and tangential $\sigma_t$ accommodation coefficients on the heat transfer coefficient $C_h$ along the frontal surface is illustrated in Fig. (3) as a function of the dimensionless height $Y$ ($\equiv y/\lambda_\infty$) for the three thicknesses investigated. According to this set of plots, it is seen that the heat transfer coefficient decreases drastically with decreasing $\alpha_n$ for the thicknesses investigated. On the other hand, no appreciable changes are observed in the heat transfer coefficient with reducing the tangential accommodation coefficient $\sigma_t$. An understanding of this behavior can be gained by considering independently the contribution of the incident $q_i$ and reflected $q_r$ heat fluxes that appear in the heat flux $q_w$ ($= q_i + q_r$). It is found (not shown) that the incident heat flux decreases as the normal accommodation coefficient $\alpha_n$ changes from 1.0 to 0.5. Nevertheless, the reflected heat flux increases for the same range of $\alpha_n$ in the frontal surface of the leading edges. As a result, the net heat flux to the body surface is significantly reduced in the frontal surface. It is also found that the incident heat flux increases slightly and the reflected heat flux decreases by a reduction in the tangential accommodation coefficient $\sigma_t$. Despite the fact that the CLL model gives a somewhat higher average velocity of scattered molecules, the tendency of decreasing the heat transfer is expected because the number of molecules colliding with the surface by unit time and unit area diminishes with incomplete accommodation.

The influence of the incomplete accommodation on the heat transfer coefficient $C_h$ along the afterbody surface is displayed in Fig. (4) as a function of the dimensionless arc length $S$ ($\equiv s/\lambda_\infty$) measured from the shoulder of the leading edge (see Fig. (2b)). Referring to Fig. (4), it is observed that the heat transfer coefficient is affected not only by changes in the normal accommodation coefficient $\alpha_n$ but also by changes in the tangential coefficient $\sigma_t$. At this time, a significant reduction in the heat transfer coefficient in the vicinity of the shoulder of the wedge is seen with decreasing the tangential accommodation coefficient $\sigma_t$, in contrast to that presented to the frontal surface. Again, by examining the contribution of the incident $q_i$ and reflected $q_r$ heat fluxes, it is

found (not shown) that both heat fluxes decrease slightly close to the stagnation region with diminishing the tangential accommodation coefficient. However, no appreciable changes are observed in the reflected heat flux.

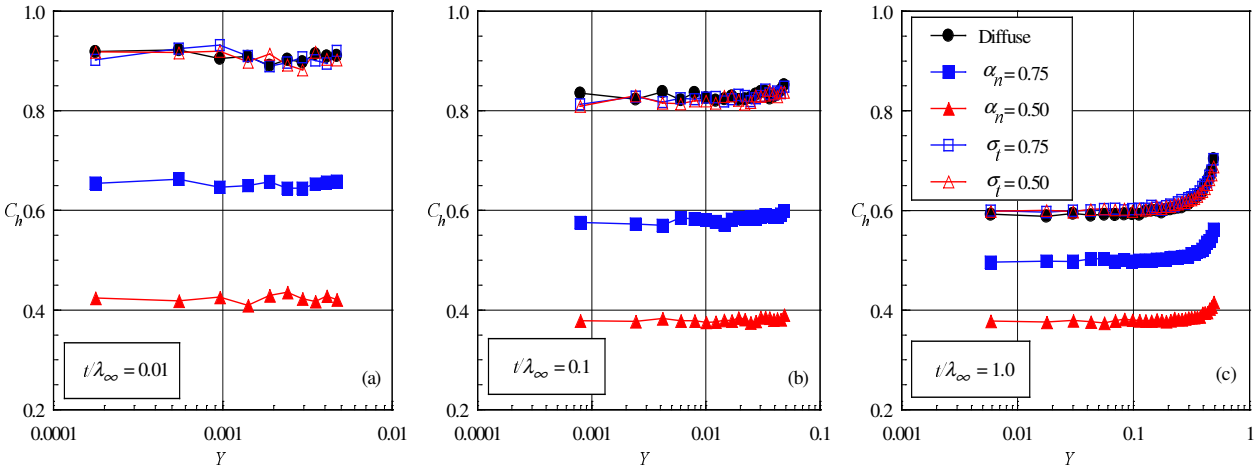


Figure 3: Heat transfer coefficient $C_h$ along the frontal surface of the wedge as a function of the accommodation coefficient. (a) $t/\lambda_\infty = 0.01$, (b) $t/\lambda_\infty = 0.1$, and (c) $t/\lambda_\infty = 1.0$ case.

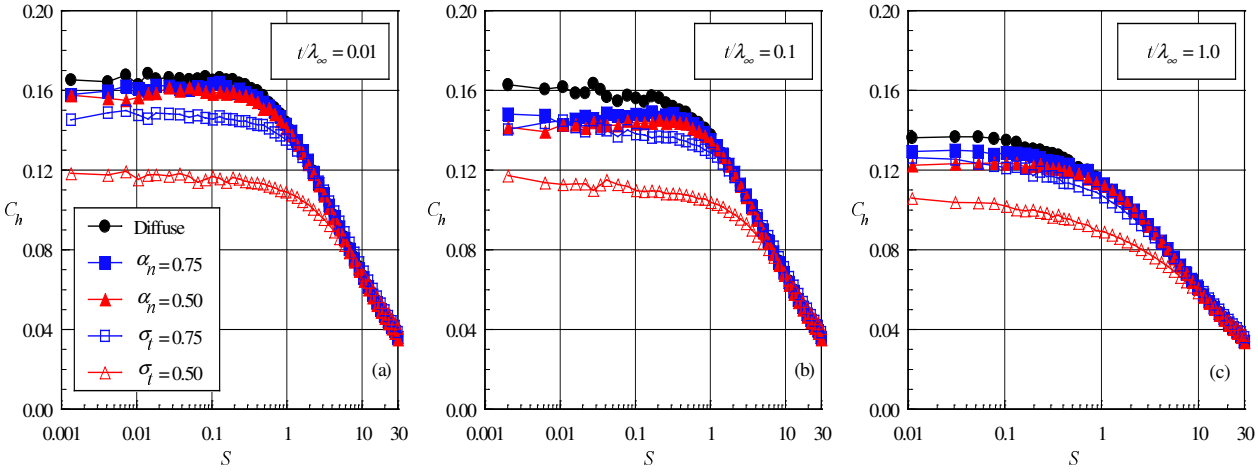


Figure 4: Heat transfer coefficient $C_h$ along the afterbody surface of the wedge as a function of the accommodation coefficient. (a) $t/\lambda_\infty = 0.01$, (b) $t/\lambda_\infty = 0.1$, and (c) $t/\lambda_\infty = 1.0$ case.

## 5.2. Total Drag Coefficient

The drag on a surface in a gas results from the interchange of momentum between the surface and the molecules colliding with the surface. The total drag is obtained by the integration of the pressure and shear stress acting on the body surface from the stagnation point of the leading edges to the tangent point common to all the leading edges (see Fig. (2a)). The total drag was obtained by assuming the shapes acting as leading edges. As a result, no base pressure effects were taken into consideration on the calculations. Results for total drag are normalized by $\frac{1}{2}\rho_\infty V_\infty^2 H$, where $H$ is the height at the matching point common to the leading edges (see Fig. (2b)), and presented in terms of total drag coefficient $C_d$ and its components of pressure drag coefficient $C_{pd}$ and the skin friction drag coefficient $C_{fd}$.

The effects of changing independently the normal and tangential accommodation coefficients on the total drag coefficient $C_d$ are shown in Tab. (3) for the thicknesses investigated. The tangential accommodation coefficient is held constant at 1.0 while the normal accommodation is varied from

1.0 to 0.5. Afterwards, the normal accommodation coefficient is held constant at 1.0 while the tangential accommodation coefficient is varied from 1.0 to 0.5. For comparison purpose, the total drag coefficient $C_d$ obtained by Santos (2002) by considering diffuse reflection is also included in this table.

Table 3: Pressure drag $C_{pd}$, skin friction drag $C_{fd}$ and total drag $C_d$ coefficients.

| | $t/\lambda_\infty = 0.01$ | | | $t/\lambda_\infty = 0.1$ | | | $t/\lambda_\infty = 1.0$ | | |
|---|---|---|---|---|---|---|---|---|---|
| | $C_{pd}$ | $C_{fd}$ | $C_d$ | $C_{pd}$ | $C_{fd}$ | $C_d$ | $C_{pd}$ | $C_{fd}$ | $C_d$ |
| *Diffuse* | 0.197 | 0.784 | 0.981 | 0.214 | 0.767 | 0.981 | 0.362 | 0.635 | 0.997 |
| $\alpha_n = 0.75$ | 0.203 | 0.794 | 0.997 | 0.221 | 0.776 | 0.996 | 0.366 | 0.644 | 1.011 |
| $\alpha_n = 0.50$ | 0.208 | 0.805 | 1.013 | 0.228 | 0.785 | 1.013 | 0.372 | 0.653 | 1.025 |
| $\sigma_t = 0.75$ | 0.180 | 0.730 | 0.911 | 0.197 | 0.713 | 0.910 | 0.346 | 0.581 | 0.928 |
| $\sigma_t = 0.50$ | 0.155 | 0.613 | 0.768 | 0.171 | 0.596 | 0.767 | 0.325 | 0.475 | 0.800 |

Referring to Tab. (3), it can be seen that variations in $\alpha_n$ or $\sigma_t$ seem to have approximately the same effect on the total drag coefficient. The total drag coefficient $C_d$ increases around 2 or 3% by a reduction in the normal accommodation coefficient, and decreases around 20% by a reduction in the tangential accommodation coefficient for the three thicknesses investigated. Figure 5 displays the dependence of the drag coefficient on the incomplete surface accommodation for the $t/\lambda_\infty = 1.0$ case. It is apparent from these set of plots that pressure drag coefficient was more affected by the incomplete surface accommodation than the skin friction drag, that was found to be not significantly different from those for complete accommodation. As was pointed out by Santos (2004), the flat-faced leading edges present distinct aerodynamic behavior in the sense that they are sharp for thicknesses $t/\lambda_\infty = 0.01$ and 0.1, and blunt for $t/\lambda_\infty = 1.0$. Moreover, they represent different degrees of rarefaction, i.e., $Kn_t$ of 100 and 10 for the two sharp leading edges and $Kn_t$ of 1 for the blunt leading edge case. In fact, the incomplete surface accommodation affects significantly the frontal and afterbody surfaces of the leading edges in different ways. However, the net effect is not so apparent.

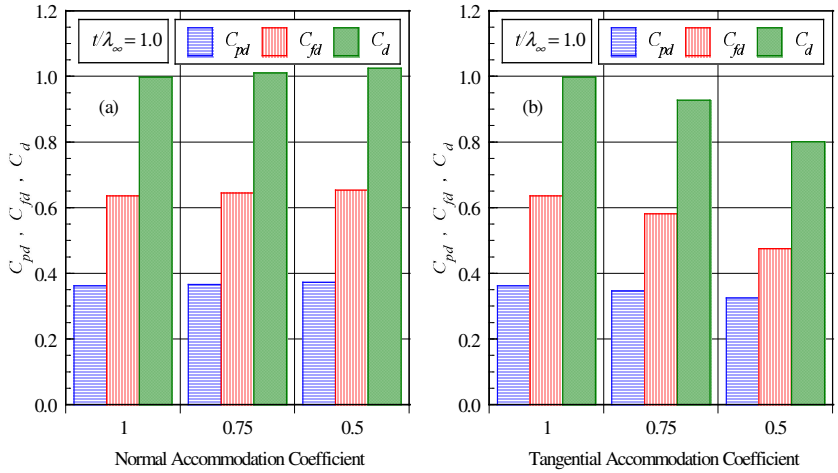


Figure 5: Comparison of pressure drag $C_{pd}$, skin friction drag $C_{fd}$ and total drag $C_d$ coefficients for the $t/\lambda_\infty = 1.0$ case. (a) Normal and (b) tangential accommodation coefficients.

One way to visualize the manner in which the two accommodation coefficients produce different behaviors is to examine the pressure and skin friction coefficients as well as the incident number flux for the leading edges. Figures 6 and 7 illustrate these properties along the frontal and afterbody surfaces, respectively, for the $t/\lambda_\infty = 0.01$ case, which corresponds to $Kn_t = 100$. In these figures, the incident number flux $N$, calculated by sampling the molecules impinging on the surface

by unit time and unit area, is normalized by the freestream number flux $n_\infty V_\infty$.

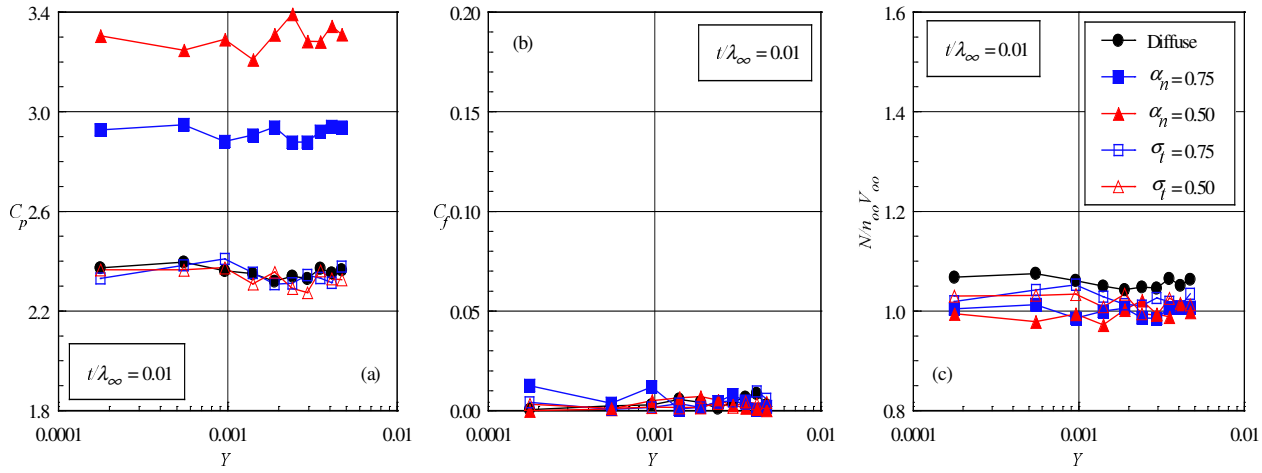


Figure 6: (a) Pressure coefficient $C_h$, (b) skin friction coefficient and (c) the incident number flux along the frontal surface of the wedge for the $t/\lambda_\infty = 0.01$ case.

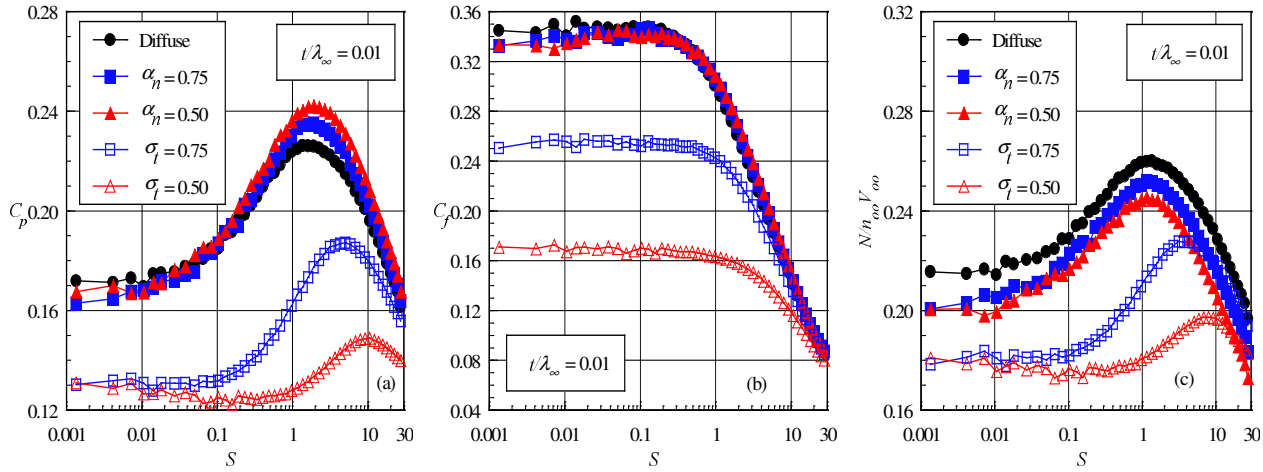


Figure 7: (a) Pressure coefficient $C_h$, (b) skin friction coefficient and (c) the incident number flux along the afterbody surface of the wedge for the $t/\lambda_\infty = 0.01$ case.

It is noted from this set of plots that pressure coefficient increases along the frontal surface by a reduction in $\alpha_n$ and diminishes considerably along the afterbody surface by a reduction in $\sigma_t$. As the thickness increases, the effect of $\alpha_n$ along the frontal surface becomes less expressive. However, a similar behavior is observed along the afterbody surface of the other wedges by a reduction in $\alpha_n$. In addition, the skin friction coefficient along the afterbody surface, which effectively contributes to the total drag, follows the same trend of the pressure in the sense that it is drastically affected by changes in $\sigma_t$. Also, it is seen that the incident number flux, i.e., the number of molecules colliding with the surface by unit time and unit area, diminishes with incomplete accommodation. Consequently, the number flux alters not only the total drag but also the heat transfer coefficient.

## 6. CONCLUDING REMARKS

This study applies the Direct Simulation Monte Carlo method to investigate rarefied gas over flat-faced leading edges. Effects of incomplete surface accommodation on the heat transfer, pressure, skin friction, and drag coefficients for a range of normal and tangential accommodation

coefficients are investigated. The normal and tangential accommodation coefficients are varied from 1.0 to 0.5, and the thickness of the frontal surface considered in this study covers hypersonic flow from the transitional flow regime to the free molecular flow.

Calculations showed that a reduction in the normal accommodation coefficient from 1.0 to 0.5 decreased the heat transfer coefficient in the vicinity of the stagnation point for the shapes investigated. In addition, a reduction in the tangential accommodation coefficient diminished the heat transfer coefficient in the vicinity of the shoulder of the leading edges on the afterbody surface. Also, it was found that the total drag coefficient is reduced by a reduction in the tangential accommodation coefficient, and increased by a reduction in the normal accommodation coefficient.

The effects of either normal or tangential accommodation coefficient showed that in order to make accurate predictions of the aerodynamic forces on, and heat transfer rates to, bodies in rarefied hypersonic flow it will be necessary to take surface accommodation into account. The calculations presented in this work have only covered a limited number of parametric variations. Further calculations with additional combinations of normal and tangential accommodation coefficients or where the internal energy accommodation is varied independently might provide more insight into the sensitivity of the aerothermodynamic quantities to gas-surface model.

## 7. REFERENCES


Bird, G. A., 1981, "Monte Carlo Simulation in an Engineering Context", Progress in Astronautics and Aeronautics: Rarefied gas Dynamics, Ed. S. S. Fisher, Vol. 74, part I, AIAA New York, pp. 239-255.

Bird, G. A., 1989, "Perception of Numerical Method in Rarefied Gasdynamics", Rarefied gas Dynamics: Theoretical and Computational Techniques, Eds. E. P. Muntz, and D. P. Weaver and D. H. Capbell, Vol. 118, AIAA, New York, pp. 374-395.

Bird, G. A., 1994, "Molecular Gas Dynamics and the Direct Simulation of Gas Flows", Oxford University Press, Oxford, England, UK.

Borgnakke, C. and Larsen, P. S., 1975, "Statistical Collision Model for Monte Carlo Simulation of Polyatomic Gas Mixture", Journal of computational Physics, Vol. 18, No. 4, pp. 405-420.

Cercignani, C., 1988, "The Boltzmann Equation and Its Applications", Springer-Verlag, New York, NY.

Cercignani, C. and Lampis, M., 1971, "Kinetic Models for Gas-Surface Interactions", Transport Theory and Statistical Physics, Vol. 1, No. 2, pp. 101-114.

Lord, R. G., 1991a, "Application of the Cercignani-Lampis Scattering Kernel to Direct Simulation Monte Carlo Method", Proceedings of the 17th International Symposium on Rarefied Gas Dynamics, Ed. A. E. Beylich, Aachen, Germany, pp. 1427-1433, July 8-14.

Lord, R. G., 1991b, "Some Extensions to the Cercignani-Lampis Gas-Surface Scattering Kernel", Physics of Fluids, Vol. A3, No. 4, pp. 706-710.

Lord, R. G., 1995, "Some Further Extensions of the Cercignani-Lampis Gas-Surface Interaction Model", Physics of Fluids, Vol. 7, No. 5, pp. 1159-1161.

Nonweiler, T. R. F., 1959, "Aerodynamic Problems of Manned Space Vehicles", J. of the Royal Aeronautical Society, Vol. 63, Sept, pp. 521-528.

Santos, W. F. N., 2002, "Truncated Leading Edge Effects on Flowfield Structure of a Wedge in Low Density Hypersonic Flight Speed", Proceedings of the 9th Brazilian Congress of Thermal Engineering and Sciences, Rio de Janeiro, RJ, Brazil.

Santos, W. F. N., 2003, "Compressibility Effects on Flowfield Structure of Truncated Leading Edge in Low Density Hypersonic Flow", Proceedings of the 17th International Congress of Mechanical Engineering, São Paulo, SP, Brazil.

Santos, W. F. N., 2004, "Flat-Faced Leading-Edge Effects in Low-Density Hypersonic Wedge Flow", Journal of Spacecraft and Rockets, (to appear, in press).

Schaaf, S. A. and Chambre, P. L., 1961, "Flow of Rarefied Gases", Princeton Aeronautical Paperbacks, Princeton University Press, Princeton, NJ.